Food Research International 173 (2023) 113363

Contents lists available at ScienceDirect

Food Research International

journal homepage: www.elsevier.com/locate/foodres

In situ extraction/encapsulation of olive leaves antioxidants in zein for improved oxidative stability of edible oils

Amarilis Santos de Carvalho [a], Anielle de Oliveira [a], Thaysa Fernandes Moya Moreira [a], Luis Gustavo Médice Arabel Costa [a], Gabrielle Donato Marcatto [a], Andre da Silva Castilhos de Melo [a], Odinei Hess Gonçalves [a,b], Maria Inês Dias [b,c], Ricardo C. Calhelha [b,c], Lillian Barros [b,c], Patricia Valderrama [a], Lucio Cardozo Filho [d], Fernanda Vitória Leimann [a,b,*]

[a] Post-Graduation Program of Food Technology (PPGTA), Federal University of Technology – Paraná – UTFPR, Campo Mourão, via Rosalina Maria dos Santos, 1233, CEP 87301-899, Campo Mourão, PR, Brazil
[b] Centro de Investigação de Montanha (CIMO), Instituto Politécnico de Bragança, Campus de Santa Apolónia, 5300-253 Bragança, Portugal
[c] Laboratório Associado para a Sustentabilidade e Tecnologia em Regiões de Montanha (SusTEC), Instituto Politécnico de Bragança, Campus de Santa Apolónia, 5300-253 Bragança, Portugal
[d] Department of Chemical Engineering, State University of Maringá – UEM, Maringá, PR, Brazil

ARTICLE INFO

Keywords:
Nanoprecipitation
Bioresidue
Cytotoxicity
Schaal Oven Test
Parafac

ABSTRACT

This study presents a sustainable and cost-effective method for preserving the bioactivity of phenolic compounds in olive leaves (OLE) during their application. The extraction and nanoencapsulation of OLE were performed in a single-step process using a rotor–stator system with zein as the encapsulating agent. The nanoprecipitation step was carried out using an aqueous sodium caseinate solution, resulting in spherical particles with an average diameter of about 640 nm, as confirmed by Transmission Electron Microscopy. Thermal characterization showed that the produced nanoparticles were more thermally stable than free OLE until 250 °C, and FTIR spectra indicated effective interaction between the phenolic compounds and zein. Antioxidant activity was evaluated using TBARS, DPPH, ABTS, and FRAP assays, with results showing that encapsulated OLE had lower antioxidant activity than free OLE. The best antioxidant capacity results were determined by TBARS assay, with IC_{50} results equal to 43 and 103 μg_{OLE}/mL for free and encapsulated OLE, respectively. No anti-inflammatory potential was detected for both samples using the RAW 264.7 model, and only free OLE showed cytotoxic activity against lung cancer and gastric carcinoma. Encapsulated and free OLE were used as antioxidants in soy, palm, and palm kernel oils and compared to BHT using Rancimat. The Schaal Oven Test was also performed, and the PARAFAC chemometric method analyzed the UV–Vis spectra, which revealed high stability of the oil when 300 mg or the nanoparticles were added per kg oil. Results suggested that zein-encapsulated olive leaf antioxidants can improve the oxidative stability of edible oils.

1. Introduction

Brazil is an emerging virgin olive oil-producing country that has been increasingly investing in olive tree cultivation (Zago et al., 2019), with about 10 000 ha cultivated with olive trees in the South and Southeast regions of the country (Crizel et al., 2020). The olive (*Olea europea* L.) leaves have been extensively used in herbal teas and food supplements. Their usage is of great interest from a food waste recovery perspective. Since olive leaves are a great source of valuable compounds such as polyphenols, they represent a rich source of potential food additives and/or nutraceuticals (Difonzo et al., 2020; Žugčić et al., 2019).

The leaves represent up to 10 wt% of the mass of the olive arriving from the fields and they must be removed from the fruits in the early steps of olive cleaning (da Rosa et al., 2019). Due to the large amount produced, more cost-effective and sustainable extraction methods to prepare olive leaf extracts (OLE) have been designed in the last few

* Corresponding author at: Post-Graduation Program of Food Technology (PPGTA), Federal University of Technology – Paraná – UTFPR, Campo Mourão, via Rosalina Maria dos Santos, 1233, CEP 87301-899, Campo Mourão, PR, Brazil.
E-mail address: fernandaleimann@utfpr.edu.br (F. Vitória Leimann).

https://doi.org/10.1016/j.foodres.2023.113363
Received 5 April 2023; Received in revised form 2 August 2023; Accepted 5 August 2023
Available online 6 August 2023

years, with the expectation of increasing profitability of olive groves and of making agricultural activity practices more sustainable (Clodoveo et al., 2021). These techniques include Supercritical Fluid Extraction (SFE) (Caballero et al., 2020), Pressurized Liquid Extraction (PLE) (Silva et al., 2022), Pulsed Electric Field extraction (PEF) (Pappas et al., 2021), and deep eutectic solvents extraction (de Almeida Pontes et al., 2021). Extraction using conventional solvents may be coupled to secondary techniques in order to improve the extraction efficiency, such as the Ultrasound-Assisted Extraction (UAE) and the Microwave Assisted Extraction (MAE) (Rosa et al., 2019). Also, the high shear homogenization extraction (HSE) that uses rotor–stator stirring systems has being reported as an effective method to extract phenolic compounds from different byproducts, such as those from red guava (Danielski et al., 2022), pinhão (Santos et al., 2018), olive leaves (Ahin et al., 2017), and others. This homogenizing system is characterized by localized high-energy dissipation and presents the advantage of being easily scaled up (Wu et al., 2019). Chee and Jawaid (2019) explained the mechanism of high shear homogenization as a powerful circumferential force created by the proximity of the outer stationary tube (stator) and the inner rotating shaft (rotor) which automatically drew the nanofiller axially into the dispersion head and then forced radially through the slots in the rotor/stator arrangement. This mechanism allows the compound extraction and the micro and nanoparticles formation.

Encapsulation techniques are helpful in preserving phenolics during storage and may provide the controlled release of the encapsulated compounds during their application (Leimann et al., 2019). The usual procedure is to first extract the target compounds and then encapsulate them in a suitable protective matrix, which dould lead to the excessive use of solvents. To overcome this disadvantage, the act of simultaneously extract and encapsulate compounds was recently proposed. Santos et al. (2020) simultaneously extracted and encapsulated curcuminoids from *Curcuma longa* L. in polyvinylpyrrolidone. The authors used a modification of the solid dispersion technique comprising a mixture of curcuma powder, solvent, surfactant, and encapsulating agent. In another approach, Mourtzinos et al. (2016) promoted the simultaneous extraction/encapsulation of olive leaves using a stoppered glass bottle submitted to stirring with water/glycerol as solvents and cyclodextrin as the encapsulating agent.

The use of device-assisted solvent extraction methods (such as high shear homogenizers or ultrassond devices) are good candidates for simultaneous extraction/encapsulation approaches, mainly because they can reach high energy dissipation (1000—10 000 m^2/s^3 and ~ 10^9 m^2/s^3, respectively, Vashisth et al., 2021). It is known that the application of high energy is a fundamental factor to the formation of interactions, such as hydrogen bonding, between encapsulation agent and the extracted compounds to be encapsulated (Karavas et al., 2006).

High shear devices have already been used in the nanoprecipitation technique to encapsulate bioactives and extracts in zein (Calliari et al., 2020; Lemes et al., 2017). Usually, zein and the compounds are solubilized in an ethanol–water solution, followed by dropwise addition of this solution into surfactant aqueous solution leading to the precipitation of zein (Pascoli et al., 2018). The application of high shear rates leads to a higher degree of supersaturation and simultaneous formation of spherical particles under decreased ethanol content (Wang & Zhang, 2019). The precipitation of zein involving the encapsulated compounds occurs due to a sequence of phenomena that include supersaturation, nucleation, growth by condensation, and growth by coagulation that leads to the formation of nanoparticles (Rivas et al., 2017).

In this work, a one-step process was proposed to nanoencapsulate the phenolics-rich extract from olive leaves aiming to reduce the operation time, as well as the use of solvents. The high shear homogenization extraction technique was carried out in the presence of zein to simultaneously extract and encapsulate the phenolic compounds under high-shear. The produced nanoparticles were incorporated into edible oils, and their potential was evaluated using the Rancimat and the Schaal Oven tests.

2. Material and methods

2.1. Material

The olive leaves were obtained from a commercial crop in Águas da Prata in Serra da Mantiqueira in São Paulo (22°00′48,6″ S 46°37′59,4″ W) and the tree species used were Arbequina, Koroneiki, and Arbosana. Zein and sodium caseinate (Sigma-Aldrich) were used in the nanoencapsulation. Soybean, palm kernel, and palm oils were used without the addition of antioxidants obtained through a donation from the COAMO cooperative. The following chemicals were also used: potassium bromide (KBr, spectroscopic grade, Sigma-Aldrich), isooctane (UV/HPLC grade, NEON), absolute ethyl alcohol (99.8%, Dynamic), BHT (99%, Scientific Exodus), ABTS (2,2′-azinobis[3-ethylbenzothiazoline-6-sulfonic acid]diammonium salt, Sigma-Aldrich), 2,2-diphenyl-1-picrylhydrazyl (DPPH, Sigma-Aldrich), potassium persulfate (Neon), hydrochloric acid (Vetec), 2,4,6-Tris(2-pyridyl)-s-triazine (TPTZ, Sigma-Aldrich), ferric chloride hexahydrate (Synth), sodium acetate (Dinâmica), glacial acetic acid (Dinâmica), ethanol (99.5%, Dinâmica).

2.2. OLE single-step extraction/nanoencapsulation

The extraction and nanoencapsulation of bioactive compounds from olive leaves followed the methodology described by Lemes et al. (2017) and Santos et al. (2018). The procedure was adapted to reduce the steps necessary to obtain the extract and subsequent encapsulation. Olive leaves (43.75 g) were milled until the formation of a coarse powder with sizes around 500 μm. Then, zein (15 g) and absolute ethanol/water (500 mL, 80:20 v/v) were added and the dispersion was kept under agitation (12,000 rpm for 15 min) in a high shear homogenizator (Ultra-turrax T25, IKA, S25N dispersion element) as described by Santos et al. (2018). After this step, the mixture was centrifuged (10 min at 5,000 rpm, Novatecnica NT825). The supernatant was collected and dripped with the aid of a burette in an aqueous solution of sodium caseinate (500 mL, 0.02 g/mL) immersed in an ice bath at 12,000 rpm to nanoprecipitation occur. The dispersion was finally dried in a circulation oven at 60 °C, collected, ground, and kept refrigerated until use. In the case of the non-encapsulated extract (olive leaf extract, OLE), it was obtained in the same proportion of leaves/ethanol/water used in the encapsulation and the same agitation in the rotor–stator, then centrifuged and the supernatant dried in an oven under the same conditions.

Two parameters were determined gravimetrically after the extraction and nanoencapsulation processes: the extraction yield (EY %) and nanoparticle production yield (NPY %). The EY corresponded to the content of extract obtained from the olive leaves. The NPY was determined by the relationship between the solids content collected at the end of the process, and the solids initially introduced (zein, sodium caseinate, and extract, determined from EY). Eqs. (1) and (2) were used, respectively, where V_t is the total volume of solvent used in the extraction (mL), m_{sa} is the mass of solids in the extract aliquot after drying (g), V_a is the volume of the extract aliquot to be dried for yield calculation (mL), m_l is the mass of leaves used in the extraction (g), m_{NP} is the dry mass of nanoparticles collected at the end of the process (g), m_s is the mass of solids (zein and sodium caseinate) used in one-step extraction/encapsulation (g), and m_E represents the mass of extract present in the leaves used for extraction/encapsulation. It is worth noting that this procedure did not differentiate between total precipitated material and the unencapsulated material.

$$EY(\%) = \left(\frac{V_t.m_{sa}}{V_a.m_l}\right).100 \quad (1)$$

$$NPY(\%) = \left(\frac{m_{NP}}{m_s + m_E}\right).100 \quad (2)$$

2.3. Characterization of OLE and OLE-containing nanoparticles

2.3.1. Phenolic compounds characterization by HPLC-DAD/ESI-MSn

The extracts were redissolved in a ethanol:water (80:20, *v/v*) solution and characterized regarding their phenolic composition using a Dionex Ultimate 3000 UHPLC (Thermo Scientific, San Jose, CA, USA) equipment (Bessada et al., 2016) with a diode array detector (DAD), programed at 280 nm and 370 nm as the preferred wavelengths, connected in line with a Linear Ion Trap LTQ XL mass spectrometer (Thermo Finnigan, San Jose, CA, USA) equipped with an ESI source working in negative mode. The Xcalibur® data system (Thermo Finnigan, San Jose, CA, USA) was used for data acquisition and analysis. The identification of the compounds was performed through the compasision with available standard compounds and using literature information regarding UV–Vis, deprotonated ion and the mass fragmentation pattern. Quantification was performed using 7-level calibration curves obtained from commercial standard compounds: apigenin-6-*C*-glucoside ($y = 107{,}025x + 61{,}531$, $R^2 = 0.9989$; LOD (Limit of Detection) = 0.19 μg/mL; LOQ (Limit of Quantification) = 0.63 μg/mL), hydroxityrosol ($y = 124154x + 17393$, $R^2 = 0.9999$, LOD = 1.22 μg/mL; LOQ = 3.68 μg/mL), naringenin ($y = 18433x + 78903$, $R^2 = 0.9998$, LOD = 0.17 μg/mL and LOQ = 0.81 μg/mL), oleuropein ($y = 32226x + 12416$; $R^2 = 0.9997$; LOD = 0.69 μg/mL and LOQ = 1.96 μg/mL), quercetin-3-*O*-glucoside ($y = 28555x + 3032.3$, $R^2 = 0.9996$, LOD = 0.02 μg/mL; LOQ = 0.07 μg/mL). The results were expressed in mg per g of extract as mean ± standard deviation.

2.3.2. Physicochemical and morphological characterization

Fourier Transform Infrared Spectroscopy (FTIR) was used to analyze the interaction between the extracted compounds and the encapsulant agent. KBr pellets were prepared with nanoparticles, free OLE, zein, sodium caseinate (NaCas), and a physical mixture (PM) of these components in the same proportion as they are present in the formulation of nanoparticles (the amount of OLE was determined by Equation 1). Samples were analyzed in IRAffinity-1 FTIR (Shimadzu Affinity-1), in the range of 4000 to 500 cm^{-1}, using 32 accumulations and a resolution of 2 cm^{-1}.

Differential Scanning Calorimetry and Thermogravimetric analyses were performed on a simultaneous thermal analyzer (STA 6000, PerkinElmer, USA). The samples (8 to 10 mg) were placed in a platinum sample holder and heated to 600 °C at 10 °C.min^{-1} under a nitrogen flux of 50 mL.min^{-1}.

Transmission Electron Microscopy (TEM) analysis was performed to evaluate the morphology of the nanoparticles. A carbon-coated copper grid (200 mesh) was prepared with a droplet deposition from a nanoparticle dispersion freshly prepared. The grid was dried, and then the sample was analyzed in a JEOL microscope model JEM 2100, at 200 kV.

The Dynamic Light Scattering (DLS) analysis was performed to determine the mean size in intensity (Dz, nm) and the Polydispersion Index (PDI, dimensionless) of the nanoparticles on a Malvern Zetasizer instrument – Nano Series. The previously dried samples were redispersed in water (0.1% w/vm, refractive index 1.333) and then analyzed.

2.3.3. Antioxidant capacity of OLE and OLE-containing nanoparticles

For all the antioxidant capacity analyses, the samples were prepared considering the amount of OLE present in the samples. Thus, for nanoparticles, the amount of OLE was calculated according to Equations 1 and 2. Results were submitted to the t-Student test at a 5% significance level ($p < 0.05$) using the Matlab software (R2021a).

DPPH as free radical: the methodology was performed following the method described by Brand-Williams et al. (1995), with some modifications. First, 10 μL of solvent (ethanol: water, 80:20 v/v) were added to 140 μL of 60 μmol.L^{-1} methanolic solution of DPPH (negative control) and 10 μL of the sample (OLE or nanoparticles at different concentrations dissolved in ethanol:water 80:20 v/v) in 140 μL of solution of DPPH (triplicate for each sample). The solutions were protected from light for 30 min, and the absorbance determinations were performed at 515 nm in the microplate reader (Thermo Plate, TP-Reader). The percentage of antioxidant activity (%AA) was determined according to Equation (3), where $ABS_{control}$ is the absorbance of the negative control and ABS_{sample} is the absorbance of the sample. The IC_{50} (mgOLE.mL^{-1}) results were obtained using the GraphPadPrism 5 software.

$$\%AA = \frac{(ABS_{control} - ABS_{sample})}{ABS_{sample}} * 100 \quad (3)$$

ABTS method: The method described by Thaipong et al. (2006) was followed with minor modifications. The working solution was prepared by mixing the following two solutions in equal amounts (20 mL each): 7.4 mmol.L^{-1} ABTS solution and 2.6 mmol.L^{-1} potassium persulfate solution. The mixture was reacted for 12 h in the dark. After this period, the working solution was prepared by adding 1 mL of this mixture to 60 mL of methanol. The absorption reading of the working solution was performed to verify if the value was close to 1.10 ± 0.02 in a UV–Vis spectrophotometer (Ocean Optics, Red Tide USB 650 UV) at 734 nm. Therefore, for the analysis itself, 150 μL of OLE solution or nanoparticles solution at different concentrations (both dissolved in ethanol:water 80:20 v/v) were mixed with 2,850 μL of the working solution in test tubes and stored in the dark for two hours. Then, the absorbance readings of the samples were taken at 734 nm. The values obtained were expressed as IC_{50} in mgOLE.mL^{-1}.

Antioxidant Power of Iron Reduction (FRAP): 5 solutions were made: 1) 40 mM hydrochloric acid solution (50 mL of distilled water, and 333 μL of HCl 37 %) were added to a volumetric flask, and then topped up with ultrapure water; 2) 10 mM TPZ solution (31.22 mg of TPTZ were dissolved in 1 mL of HCl), and this solution was completed with HCl to a volume of 10 mL; 3) 20 mM ferric chloride solution (0.3344 g of ferric chloride hexahydrate were dissolved in 100 mL of distilled water); 4) 0.3 M sodium acetate buffer with pH 3.6 (0.755 g of sodium acetate was dissolved in 230 mL of ultrapure water), the pH was adjusted to 3.6 with glacial acetic acid gradually, the solution was transferred to a 250 mL volumetric flask with distilled water and the pH was checked. 5) Complex-Ferric (5 mL of 10 mM TPTZ solution, 4 mL of 20 mM ferric chloride solution, and 50 mL of 0.3 M sodium acetate buffer). For the analysis, 100 μL of the sample (0.406 mgOLE.mL^{-1} or 2.800 mgNP.mL^{-1}, equivalent amount of nanoparticles to the free OLE in ethanol: water 80:20 v/v) were added to 370 μL of distilled water and 3000 μL of the ferric complex for sample preparation, and 470 μL of distilled water and 3000 μL of the ferric complex for the control. The tubes were shaken and placed in a bath at 37 °C for 30 min. All the procedure was performed with the lights off. The spectra were read in UV–Vis at 595 nm, and the results were expressed as $\mu mol_{ET}.g_{OLE}^{-1}$.

Thiobarbituric acid reactive substances (TBARS) formation inhibition assay: The capacity of free and nanoencapsulated OLE to inhibit the formation of thiobarbituric acid reactive substances (TBARS), such as malondialdehyde generated from the *ex vivo* decomposition of lipid peroxidation products, was evaluated using porcine brain cell homogenates, following the method described previously by Pinela et al. (2012). Trolox was used as a positive control. The results were expressed as IC_{50} values (μg.mL^{-1}), i.e. the sample concentration providing 50% of antioxidant activity.

2.3.4. Cytotoxic and anti-inflammatory activity

The following human tumor cell lines were used for cytotoxic potential evaluation of OLE and nanoparticles: AGS (gastric adenocarcinoma), CaCo (colorectal adenocarcinoma), MCF-7 (breast adenocarcinoma), NCI-H460 (lung carcinoma). A non-tumor cell line was also tested: PLP-2 (primary pig liver culture). All of them were maintained in RPMI-1640 medium supplemented with 10% fetal bovine serum, glutamine (2 mM), penicillin (100 U.mL^{-1}), and streptomycin (100 mg.mL^{-1}), with the exception of PLP2, maintained in DMEM

medium supplemented with fetal bovine serum (10%), glutamine (1%) and antibiotics (1%). The culture flasks were incubated in an incubator at 37 °C and with 5% CO_2, under a humid atmosphere. The cells were used only when they had 70 to 80% confluence. A known mass of OLE or nanoparticles (8 mg) was dispersed in H_2O (1 mL), to obtain the stock solutions with a concentration of 8 mg.mL^{-1}, and then water was further added to adjust the concentration to 0.125——8 mg.mL^{-1}. Each extract concentration (10 μL) was incubated with the cell suspension (190 μL) of the cell lines tested in 96-well microplates for 72 h. The microplates were incubated at 37 °C and with 5% CO_2, in a humid atmosphere, after checking the adherence of the cells. All cell lines are tested at a concentration of 10,000 cells/well. After the incubation period, the cells were corrected: TCA (10% w/v; 100 μL) was previously cooled, and plates were incubated for 1 h at 4 °C, washed with water, and, after drying, an SRB solution (0.057%, m/v; 100 μL) was added, left to stand at room temperature for 30 min. To remove non-adhered SRB, plates were washed three times with acetic acid (1% v/v) and placed to dry. Finally, an adhered SRB was solubilized with Tris (10 mM, 200 μL), and the absorbance at a wavelength of 540 nm was read in the Biotek ELX800 microplate reader. The results are expressed in terms of the concentration of the sample with the ability to inhibit cell growth by 50% (GI_{50}), and ellipticine was used as a positive control.

The anti-inflammatory activity was determined as follows. The OLE or nanoparticles were dispersed in H_2O to obtain a final 8 mg.mL^{-1} dispersion. Then water was added to obtain the concentrations to be tested (0.125–8 mg.mL^{-1}). The RAW 264.7 mouse macrophage cell line, obtained from DMSMZ - Leibniz - Institut DSMZ - Deutsche Sammlung von Mikroorganismen und Zellkulturen GmbH, was grown in DMEM medium, supplemented with heat-inactivated (SFB) fetal serum (10%), glutamine and antibiotics, and kept in an incubator at 37 °C, with 5% CO_2 and under a humid atmosphere. Cells were detached with a cell scraper. An aliquot of the cell suspension of macrophages (300 μL) with a cell density of 5×10^5 cells.mL^{-1} and a proportion of dead cells below 5%, according to the Trypan blue exclusion test, was placed in each well. The microplate was incubated for 24 h in the incubator with the previously indicated conditions to allow adequate cell adherence and multiplication. After that period, the cells were treated with different concentrations of OLE or nanoparticles (15 μL, 0.125——8 mg.mL^{-1}) and incubated for one hour, with the range of concentrations tested being 6.25——400 μg.mL^{-1}. Stimulation was performed by adding 30 μL of the liposaccharide solution - LPS (1 mL.mL^{-1}) and incubating for 24 h. Dexamethasone (50 mM) was used as a positive control, and samples without LPS were used as a negative control. Nitric oxide was quantified using a Griess reagent system kit (nitrophenamide, ethylenediamine, and nitrite solutions) and through the nitrite calibration curve (100 mM sodium nitrite at 1.6 mM) prepared in a 96-well plate. The nitric oxide produced was determined by reading absorbances at 540 nm (ELX800 Biotek microplate reader, Bio-Tek Instruments, Inc., Winooski, VT, USA) and compared with the standard calibration line. The results were calculated through the graphical representation of the percentage of inhibition of nitric oxide production versus the sample concentration and expressed in relation to the concentration of each of OLE or nanoparticles that causes the 50% inhibition of nitric oxide production (IC_{50}).

2.4. Application of OLE and nanoparticles as natural antioxidants for edible oils

2.4.1. Oil samples preparation

OLE, nanoparticles, and the synthetic antioxidant BHT were added to palm, palm kernel, and soybean oils. The concentration of antioxidants was defined based on the recommendation of the Brazilian Regulatory Agency RDC n° 281 (ANVISA, 2019). BHT concentration used as 300 mg.kg$_{oil}^{-1}$. Oil samples were heated to 40 °C and then nanoparticles were added at 0, 150, 300, and 450 mg$_{NP}$.kg$_{oil}^{-1}$. Oils containing free OLE were also obtained containing 47, 94, and 141 mg$_{OLE}$.kg$_{oil}^{-1}$ (OLE was added to match the OLE concentration in the nanoparticles).

2.4.2. Oil analysis and stability

Gas Chromatography (GC) was used to determine the fatty acids profile. Methyl tricosanoate (23:0, Sigma-Aldrich) was used as an internal standard according to Hartman and Lago methodology (Milinsk et al., 2008). Fatty acid methyl esters (FAMEs) were separated, identified, and quantified using chromatography standards (Sigma-Aldrich, F. A.M.E. Mix C14-C22) (Joseph & Ackman, 1992). Transesterifications were performed in triplicate.

The oxidative stability of the oils was evaluated by Rancimat (892 Professional Rancimat, Metrohm) to determine their induction time (h). Measurements were done with 3 g of each oil sample at 131 °C under an oxygen flow of 20 L.h^{-1}. The procedure was performed in duplicate and results were submitted to analysis of variance (ANOVA) and Tukey's test at a 5% significance level ($p < 0.05$) using the Matlab program (R2021a, MathWorks).

The Schaal Oven Test was used to evaluate the accelerated stability of the palm kernel oil containing nanoparticles at 150 and 300 mg$_{NP}$.kg$_{oil}^{-1}$ and BHT at 300 mg.kg$_{oil}^{-1}$. Samples were placed in open Eppendorf tubes (2 mL), in duplicate, and taken to the oven for seven days at 60 °C (Guimarães-Inácio et al., 2018). Solutions of the oil in isooctane (1:1000 v:v) were obtained and filtered with hydrophilic PTFE syringe filters (0.45 μm) and analyzed daily in a UV–Vis Spectrophotometer using a quartz cuvette with 1 cm light path. A baseline correction algorithm was applied to each spectrum (Matlab R2021a software, MathWorks). Data were organized in a three-dimensional tensor format, and the PARAFAC chemometric tool was applied (Rosa et al., 2019). The PARAFAC is a multivariate calibration method used to determine an analyte in situations where interferents are present in the sample. It allows modeling the interferents together with the analyte of interest, replacing the physical separation of the species with a chemometric separation of the signals. The advantages of this method include speed, reduction in the use of reagents, low cost, and simplification in sample preparation, which reduces possible errors caused by manipulation. PARAFAC is a generalization of PCA for multidimensional data and a restricted version of the Tucker method. It is less flexible and uses fewer degrees of freedom, making it suitable for modeling systems with factors related to physicochemical laws (Sena et al., 2005).

3. Results and discussion

3.1. OLE and nanoparticles characterization

Table 1 presents the quantification of the phenolic compounds presented in the olive leaf extract (OLE).

The most abundant phenolics found were isorhamnetin, quercetin, luteolin, and isorhamnetin and the total phenolic compounds was 12.566 ± 0.256 mg.g$_{extract}^{-1}$. The phenolic compounds found in the extract was very similar to that previously reported (da Silva et al., 2022; D'Antuono et al., 2014; Li et al., 2017; Llorent-Martínez et al., 2015; Sanz et al., 2012).

The leaf extraction yield (EY %) and in situ nanoencapsulation yield (NPY %) found were 27 ± 3% of extract to the leaves mass (or 29 ± 3 % on a dry basis), and 69 ± 4%, respectively. Şahin and Şamlı (2013) found an extraction yield of 20.1 % (201.2 mg of extract per gram of dried olive leaf) and concluded that the hydroethanolic solvent (50:50) resulted in a greater extraction yield than pure ethanol. Coppa et al. (2017) found an extraction yield of 25.9 ± 0.6 % using water/ethanol (30/70) as solvent by dynamic maceration. The extraction yield found in the present work was higher than that found by other authors, probably due to the different origins of the leaves, as well as the high shear promoted by the rotor–stator system (Santos et al., 2018). Furthermore, the NPY probably is not close to 100% because part of zein was removed with the residual leaves during centrifugation. The interaction between zein and lignin (that is part of the leaves) was already reported by Oliviero et al. (2011), who identified these interactions by infrared spectroscopy and X-ray diffraction.

Table 1
Chromatographic and mass responses, tentative identification, and quantification (mg.$g^{-1}_{extract}$) of the phenolic compounds found in olive leaf extracts.

Peak	Rt (min)	λmax (nm)	$[M-H]^-$ (*m/z*)	MS^2 (*m/z*)	Tentative identification	Quantification (mg.$g^{-1}_{extract}$)
1	4.19	281	315	153(100),123(5)	Hydroxytyrosol glucoside	0.0369 ± 0.0004
2	5.38	281	153	123(100)	Hydroxytyrosol	0.0285 ± 0.0001
3	9.53	324	593	503(29),473(100),383(12),353(22),325(5)	Apigenin-6-*C*-hexoside-8-*C*-hexoside	tr
4	11.95	285	639	621(100),529(15),459(7),179(5)	*β*-Hydroxyverbascoside diastereoisome	0.00252 ± 0.00001
5	13.28	344	609	301(100)	Quercetin-*O*-deoxyhexosyl-hexoside	0.943 ± 0.003
6	15.22	281	525	481(100),389(28),345(20),19589),165(18)	Demethyloleuropein	0.143 ± 0.003
7	16.54	285,329	449	287(100)	Eriodictyol-*O*-hexoside	0.618 ± 0.021
8	16.66	329	623	461(100),315(10)	Isorhamnetin-*O*-hexoside-*O*-rhamnoside	1.288 ± 0.022
9	17.35	334	739	593(100),285(23)	Luteolin-O-deoxyhexosyl-O-deoxyhexosylhexoside	0.6944 ± 0.0003
10	17.62	344	609	301(100)	Quercetin-3-*O*-rutinoside	2.108 ± 0.045
11	18.03	347	593	285(100)	Luteolin-*O*-deoxyhexoside-hexoside	1.988 ± 0.055
12	19.2	345	447	285(100)	Luteolin-*O*-hexoside	3.256 ± 0.16
13	20.74	324	701	539(100),377(10),307(5)	Oleuropein hexoside isomer I	0.027 ± 0.001
14	21.71	332	623	315(10)	Isorhamnetin-*O*-deoxyhexoside-hexoside	0.9 ± 0.008
15	23.67	335	701	539(21),377(100),307(79)	Oleuropein hexoside isomer II	0.176 ± 0.007
16	24.64	333	539	377(100),307(43),197(5),153(5)	Oleuropein	0.345 ± 0.006
17	25.01	339	539	377(100),307(37),197(5),153(5)	Oleuropein isomer I	0.0052 ± 0.0004
18	28.35	328	583	537(100),403(94),223(9),151(5)	Lucidumoside C	0.006 ± 0.0002
Total Phenolic Acids						0.0654 ± 0.0005
Total Iridoid Glucosides						0.704 ± 0.008
Total Flavonoids						11.796 ± 0.263
Total Phenolic Compounds						12.566 ± 0.256

tr – trace amounts. Standard Calibration curves used for quantfiication: apigenin-6-*C*-glucoside ($y = 107{,}025x + 61{,}531$, $R^2 = 0.9989$; LOD = 0.19 μg/mL; LOQ = 0.63 μg/mL, peak 3), hydroxityrosol ($y = 124154x + 17393$, $R^2 = 0.9999$, LOD = 1.22 μg/mL; LOQ = 3.68 μg/mL, peak 1 and 2), naringenin ($y = 18433x + 78903$, $R^2 = 0.9998$, LOD = 0.17 μg/mL and LOQ = 0.81 μg/mL, peak 7), oleuropein ($y = 32226x + 12416$; $R^2 = 0.9997$; LOD = 0.69 μg/mL and LOQ = 1.96 μg/mL, peaks 4, 6, 13, 15, 16, 17, and 18), quercetin-3-*O*-glucoside ($y = 28555x + 3032.3$, $R^2 = 0.9996$, LOD = 0.02 μg/mL; LOQ = 0.07 μg/mL, peaks 5, 8, 9, 10, 11, 12, and 14).

The visual aspect of the olive leaves used in this work, the OLE, and the nanoparticles can be observed in Fig. 1. Images obtained by Transmission Electron Microscopy (TEM) are presented in Fig. 2.

DLS analysis of nanoparticles indicated a polydispersity index (PDI) of 0.9 ± 0.1 and an average intensity diameter Dz equal to 638.5 ± 55.8 nm, which may be considered a wide distribution (Leimann et al., 2013, Cháirez-Ramírez et al., 2015). However, a careful inspection of the microscope images demonstrated that the larger particles may actually be clusters of smaller particles, which could explain the large values of PDI and average sizes found. Such results are greater than those reported

Fig. 1. (A) Olive leaves used in this work, varieties (I) Arbequina, (II) Arbosana, and (III) Koroneik; (B) zein nanoparticles containing OLE; and (C) Olive leaf extract (OLE).

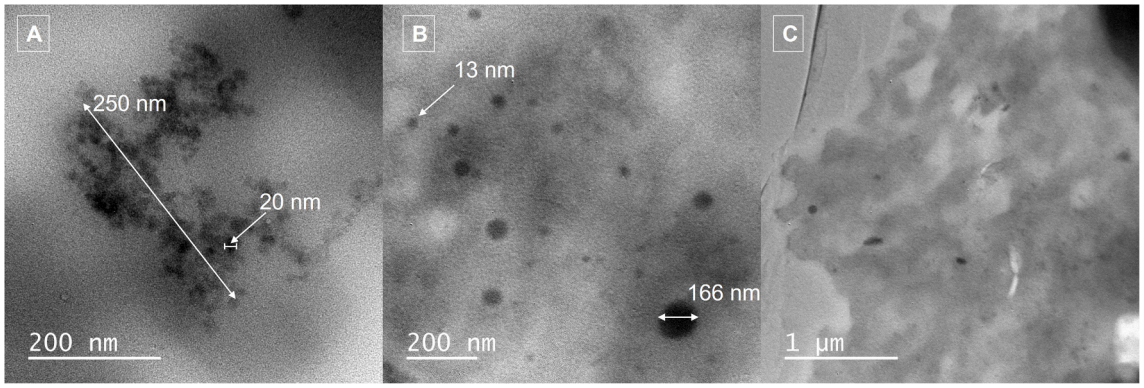

Fig. 2. Transmission Electron Microscopy (TEM) images of zein OLE-loaded nanoparticles.

by Lemes et al. (2017) in the nanoencapsulation of curcumin in zein by the same technique (Dz equal to 190 ± 2 nm and PDI of 0.25 ± 0.01). Calliari et al. (2020) encapsulated hibiscus extract in zein, also by nanoprecipitation, and found values equal to 216 ± 27 nm and 0.25 ± 0.02 for Dz and PDI, respectively. The difference is probably due to the fact that zein possibly interacted differently with the extracted compounds and the olive leaves during the in situ extraction/encapsulation process.

Nanoparticles presented spherical structures and sizes ranging from 13 to 170 nm, and the presence of large aggregates composed by smaller nanoparticles was also detected. For instance, a cluster of approximately 250 nm formed by smaller nanoparticles in the range of 20 nm may be seen in Fig. 2 (A). Also, a large cluster of approximately 12 μm can be observed in Fig. 2 (C). do Prado Silva et al. (2017) found a very similar morphology and sizes (between 80 and 600 nm) to those presented in Fig. 2 in the encapsulation of lutein using the same nanoencapsulation technique, wall material (zein), and surfactant (sodium caseinate).

Fig. 3 presents the FTIR spectra of the analyzed samples. For all samples, the characteristic band of hydroxyl groups (–OH) was identified (3600 to 3000 cm^{-1}). Also, the –CH stretch typical band was found at approximately 2920 cm^{-1}. Other bands identified in the analyzed spectra were: around 1530 cm^{-1}, probably referring to C = O bonds; 1250 cm^{-1}, related to C-N stretching and N–H (amide) bending combination; and 1080 cm^{-1} referred to stretching of C-O-C bonds (Deng et al., 2019).

For the zein sample, the bands found at 1633 cm^{-1}, and 1520 cm^{-1} are characteristics of amides I and amide II of β-sheet structures (Zhu et al., 2021). Hajjari et al. (2021) found similar results for bands related to amide (N–H) groups (1645, 1517, and 1447 cm^{-1}), and for the C–H elongation (2930 cm^{-1}).

The FTIR results showed for nanoparticles sample a reduction in the intensity of the hydroxyl characteristic bands from the antioxidant compounds from olive leaf extract (3420 cm^{-1}), as well as the –NH group of zein (1651 cm^{-1}), when compared to pure zein and MF, indicating reticulation of zein by hydrogen bonding interaction with the extract. Erdogan, Demir and Bayraktar (2015) produced electrospun zein fibers containing olive leaf extract. The authors found the same results seen in the present work, indicating that the crosslinking of zein occurred due to the interaction with the polyphenolic compounds of the extract. The same effect has been observed by other authors who encapsulated other extracts containing polyphenols in proteins such as gelatin (Zhao & Sun, 2017) and isolated protein from soybean (Souza et al., 2020). Also, this reinforces the hypothesis that the interaction between the components during the extraction/encapsulation process may have affected the size of the nanoparticles.

The reduction in the intensity of bands located at 2851 and 2928 cm^{-1} (stretch –CH) may indicate the creation of a zein layer over the extract. The same was verified for this region in work by de Souza Tavares et al. (2021) for a similar intensity reduction for zein

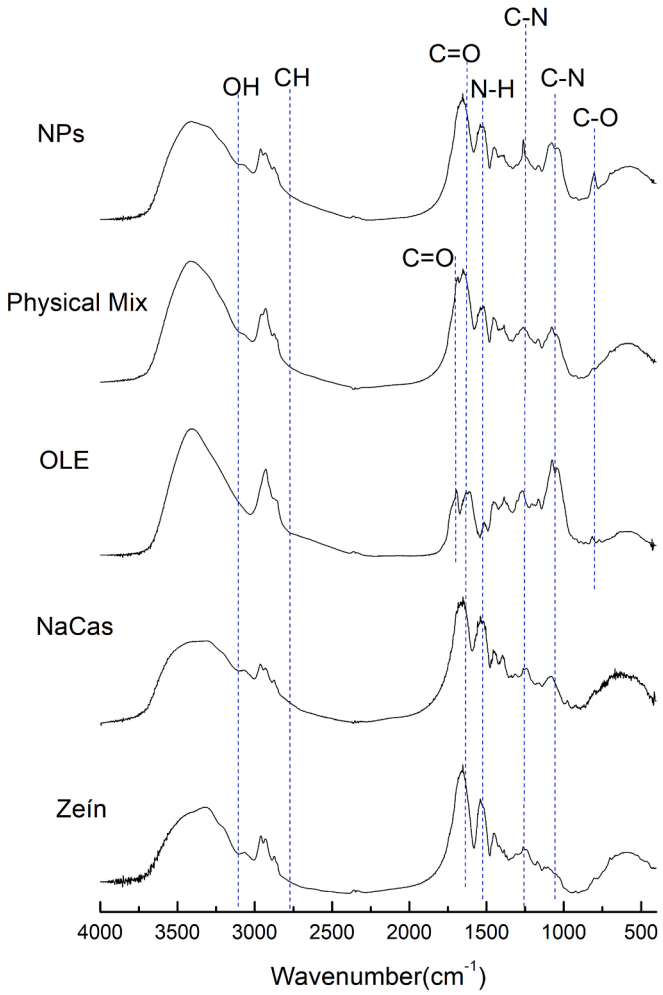

Fig. 3. FTIR spectra of free OLE, sodium caseinate (NaCas), zein, physical mixture of the components and OLE-loaded nanoparticles (NPs).

nanocapsules loaded with *Origanum vulgare* Linneus and *Thymus vulgaris* that had their bands shifted by 2966 cm^{-1} (blank particles) for 2959 cm^{-1}.

For the free extract (OLE), the band located at 1700 cm^{-1} related to C = O present in phenolic compounds was found. When analyzing the physical mixture, it was possible to observe an increase in the intensity of this band due to C = O bonds from zein and sodium caseinate (NaCas). Comparing the physical mixture with the nanoparticles, the intensity of the bands presented in the region between 1500 and 1700 cm^{-1}

increased, possibly due to strong interactions of OLE compounds with amide I and II zein groups. The same behavior may be observed for the band close to 800 cm^{-1}, probably referring to C-O bonds. Rikhtehgaran et al. (2021a), who encapsulated OLE in caseinate micelles, described the same behavior and stated that encapsulation affects the conformational changes in the encapsulating agent, leading to the formation of new bonds between the nanocarrier and OLE constituents.

The DSC curves of the samples are presented in Fig. 4. Zein showed a thermal transition onset at 66 °C and degradation starting from 173 °C. Hajjari et al. (2021) reported the degradation of zein between 250 and 450 °C and explained it by the degradation of protein internal covalent bonds. Furthermore, they found a thermal transition for zein between 143 and 186 °C and attributed this temperature to a glass transition (Tg). In the present work, the transition started at 173 °C, a value within the Tg range indicated by Feng et al. (2020). However, the degradation temperature was not visible. These variations may be associated with the corn variety from which the zein was extracted, the cultivation location, and the treatment conditions. All these conditions may interfere with the polymer's structure and, consequently, its thermal degradation temperature.

The olive leaf extract (OLE) presented a thermal transition starting at approximately 150 °C. The physical mixture sample of components present in nanoparticles formulation (zein, sodium caseinate, and extract) showed a peak temperature at 173 °C, the same point found for pure zein. Nanoparticles presented the transition onset at 250 °C. As de Souza Tavares et al. (2021) reported, phenolic compounds are prone to form hydrogen bonds with the structure of zein. Thus, it is possible that there was cross-linking between the phenolic compounds of OLE and zein, increasing the thermal stability and indicating the three-dimensional structure formation. Furthermore, it was possible to detect the degradation temperature of the extract in the physical mixture, which was not observed in the nanoparticles. González-Ortega et al. (2020) microencapsulated the olive leaf extract in maltodextrin and trehalose by freeze-drying and found thermal events between 111 and 175 °C. This may indicate that the nanoparticles prepared in the present work are more thermally stable since they started to degrade at 250 °C.

The TGA curves are shown in Fig. 5, and the 1st derivatives (DTGA) were also plotted for each sample. The residual mass at the end of the analysis (600 °C) was 18.3 % for zein, 22 % for the physical mixture, and 29.6 % for the nanoparticles. Moreno et al. (2019) found 17 % of residual mass for electrospun pure zein fibers at 600 °C. The increase in the residual mass in the nanoparticles sample may indicate a greater resistance to degradation, which may be due to the crosslink between zein with the polyphenolic compounds of the extract (Erdogan et al., 2015), which corroborates the FTIR results. It became more evident DTGA curves that the beginning of OLE thermal degradation was at 150 °C with a maximum of 200 °C. Also, the maximum degradation temperatures for zein, physical mixture, and nanoparticles were detected at 324, 311, and 311 °C, respectively. Hajjari et al. (2021) found thermal degradation for zein between 47 and 85 °C (moisture loss) and 295 and 354 °C and explained it by the degradation of the internal covalent bonds of the zein. Although the signals were relatively reduced in the nanoparticles sample, the DTGA curves showed a mass loss peak in a higher temperature when compared to the OLE sample, suggesting the interaction between the OLE components and the zein and an increase in the thermal stability.

3.2. Antioxidant, cytotoxic, and anti-inflammatory activity of OLE and OLE-loaded nanoparticles

Table 2 presents the antioxidant capacity by DPPH, ABTS, FRAP and TBARS results of free OLE and the nanoencapsulated extract.

The free extract (OLE) showed higher antioxidant capacity when compared to the nanoencapsulated extract. It was also found that the concentration of both OLE and nanoparticles was much lower for inhibiting free radical scavenging for ABTS than DPPH. Azar et al. (2021) nanoescapsulated the olive leaf extract in a liquid–liquid emulsion (a water-soluble extract). The DPPH analysis was performed on days 1 and 30 to verify the antioxidant activity over the storage time (0.5 $g_{sample}.mL^{-1}$), resulting in antioxidant activities equal to 90 and 87 %, respectively. On the other hand, the authors found a reduction in the antioxidant activity equivalent to 6 % for the free extract after 30 days of storage. They justified this behavior by nanocapsules' gradual release of the antioxidant compounds. Rikhtehgaran et al. (2021b), who performed a release test for casein nanoparticles containing olive leaf extract in three fatty food simulants, reported that the release rate was lower in the first three hours. After these initial hours, the release was gradual (total analysis time of 90 h).

Lins et al. (2018) carried out a study on olive leaves a pre-extraction in soxhlet with n-hexane to remove hydrophobic compounds. Then extraction was carried out in methanol:water (80:20 v/v), and the IC_{50} for ABTS was found at a concentration of 16.1 ± 1.2 $\mu g.mL^{-1}$, which is higher than those presented here. However, they used methanol:water solution as extraction solvent, resulting in the extraction of different phenolic compounds but may also offer toxicity if residuals are ingested.

The FRAP results corroborated the antioxidant capacities determined by ABTS and DPPH, indicating in this case that OLE has an antioxidant

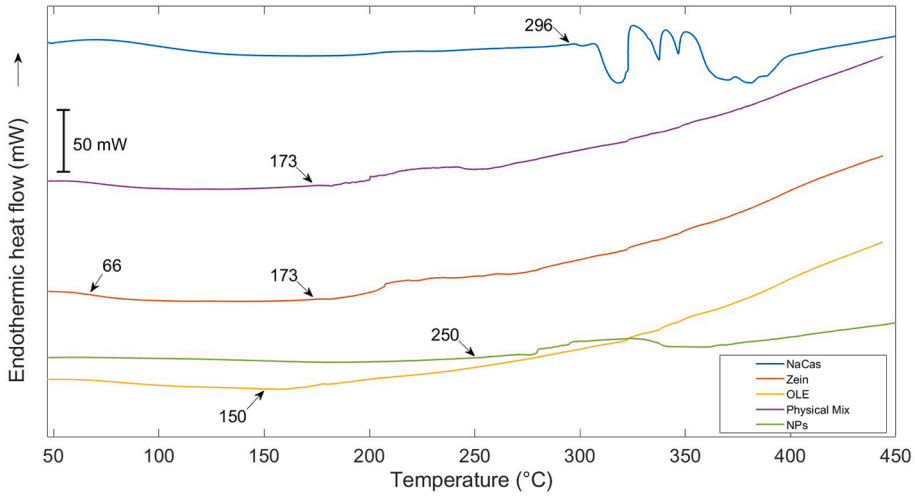

Fig. 4. DSC curves of OLE, OLE-loaded nanoparticles (NPs), zein, sodium caseinate (NaCas), and physical mixture (physical mix) of the three components (OLE, zein, and NaCas).

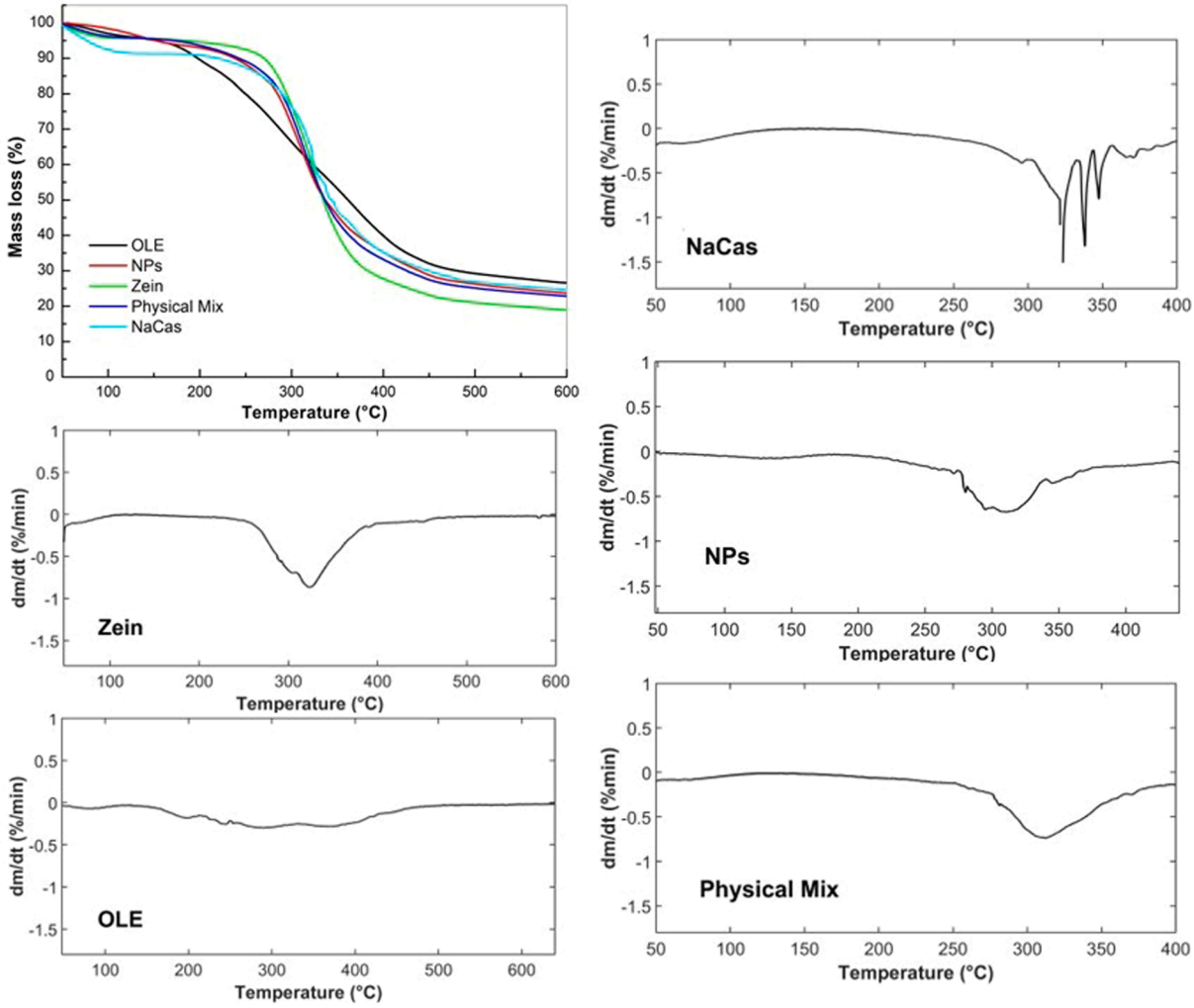

Fig. 5. A) Mass loss curves obtained by TGA of samples of OLE, NPS containing OLE, zein, sodium caseinate (NaCas), and physical mixture of the three components (OLE, zein, and NaCas). DTGA curves: B) zein; C) OLE, D) sodium caseinate (NaCas); E) physical mixture; and F) OLE-loaded nanoparticles.

Table 2
Antioxidant capacity of samples by DPPH, ABTS, and TBARS expressed in IC_{50} and FRAP in μmol Trolox equivalent (TE) per gram of OLE in the sample.

	OLE	OLE-loaded nanoparticles
DPPH IC_{50} ($mgOLE.mL^{-1}$)	$0.597^{a} \pm 0.009$	$0.803^{b} \pm 0.008$
ABTS IC_{50} ($mgOLE.mL^{-1}$)	$0.136^{a} \pm 0.015$	$0.216^{b} \pm 0.001$
FRAP ($\mu mol_{ET}.g^{-1}_{OLE}$)	$4250^{b} \pm 26$	$132^{a} \pm 6$
TBARS IC_{50} ($\mu g.mL^{-1}$)	$43^{a} \pm 3$	$103^{b} \pm 2$

[a,b] Average results followed by a different letter in the same row indicate a significant difference in the t-Student test ($p < 0.05$). IC_{50} values correspond to the extract concentration needed to inhibit by 50% the formation of thiobarbituric acid reactive substances (TBARS), Trolox: 9.1 ± 0.3 μg/mL.

approximately ten times greater than nanoencapsulated OLE. Lins et al. (2018) reported the antioxidant capacity of olive leaf extract (where was used the solvent methanol/water, 80:20 v/v) in the extraction), by FRAP assay, equal to 281.8 ± 22.8 $mg_{TE}.g^{-1}$. The difference in antioxidant activity between olive leaf extracts can still be justified by harvesting the leaves, their species, or even soil conditions and growing region, which may be more conducive to content development antioxidants (Lins et al.. 2018). Elnahas et al. (2021) reported that the genotype strongly influences olive leaf extract's phytochemical composition and content.

Table 3 presents the anti-inflammatory and cytotoxic activity results for free and nanoencapsulated OLE. It can be noted that no anti-inflammatory activity was detected below 400 $\mu g.mL^{-1}$. The only cytotoxic effect found was for free OLE against AGS (gastric carcinoma) and NCI-H460 (lung cancer), being more effective against gastric carcinoma.

Table 3
Anti-inflammatory and cytotoxic activities of free and OLE-loaded nanoparticles.

	OLE	OLE-loaded nanoparticles
Anti-inflammatory activity IC_{50} (μg.mL^{-1})		
RAW 264.7	> 400	> 400
Cytotoxicity IC_{50} (μg.mL^{-1})		
AGSGastric carcinoma	231 ± 14	> 400
CaCo2Colon adenocarcinoma	> 400	> 400
MCF-7Breast carcinoma	> 400	> 400
NCI-H460Lung cancer	294 ± 15	> 400
PLP-2Non-tumor cell line (primary pig liver culture)	> 400	> 400

IC_{50} values for Dexamethasone: 6.3 ± 0.4 μg/mL (RAW 264.7). GI_{50} values for Ellipticine: 1.23 ± 0.03 μg/mL (AGS), 1.21 ± 0.02 μg/mL (Caco- 2), 1.02 ± 0.02 μg/mL (MCF-7), 1.02 ± 0.01 μg/mL (NCI-H460), 1.4 ± 0.1 μg/ mL (PLP2).

3.3. Application of OLE and nanoparticles as natural antioxidants for edible oils

3.3.1. Oils characterzation and Rancimat test

The OLE and the nanoparticles were added to palm oil, palm kernel oil, and soybean oil (fat acids profiles of the oils are presented in Table S1, Supplementary Material). Fig. 6 presents the results for the induction time determined by the Rancimat method for the oils.

It is worh noting that the nanoparticles are essentially insoluble in the oils, forming a opaque colloidal dispersion when added. The highest stability determined by Rancimat was obtained for palm kernel oil, which presented the highest amount of saturated fatty acids (Table S1, Supplementary Material). The unsaturated fatty acids (UFA) results follow the same trend as the induction time of the oils. Regarding the soybean oil samples, none of the samples containing OLE (free or encapsulated) showed statistical similarity with the oil containing BHT. Samples added with free or nanoencapsulated OLE were statistically equal with the control sample (no antioxidant added), except for those added with nanoparticles at 47 $mg_{OLE}.kg_{oil}^{-1}$. Thus, it can be concluded that at the concentrations evaluated, free and nanoencapsulated OLE could not improve the oxidative stability of soybean oil.

Mohammadi et al. (2016) prepared nanoemulsions with the olive leaves extract (stabilized with whey protein concentrate and pectin) and applied it to soybean oil at 100, 200, and 300 $mg_{nanoparticles}/kg_{oil}$, as well as the free extract separately. The authors demonstrated by the Rancimat analysis that free olive leaf extract resulted in a longer induction time and explained this fact by the hindered effect caused by the protection promoted by the biopolymers layer around the dispersed emulsion droplets that covers the antioxidants.

Results for palm oil showed the best oxidative stability for the sample containing free OLE at a concentration of 141 mgOLE.kg^{-1} (8.51 h), when compared to BHT. Considering that the extract concentration is half of the BHT concentration used, this result shows a significant effect of the antioxidant action of the extract. Also, the samples that were added with nanoparticles at 141 mgOLE.kg^{-1} and free OLE at 94 mgOLE.kg^{-1} presented better oxidative stability than the control palm oil sample.

Salta et al. (2007) applied the OLE (obtained by extraction with methanol) to palm oil at a concentration of 200 mg of total polyphenols (determined by Folin–Ciocalteau assay) per kg of oil. The authors observed an increase in the induction time from 17 h to 21 h when the extract was added (Rancimat assay at 110° and 20 L.h^{-1} of air flow). Chiou et al. (2009) fried potatoes with palm oil enriched with OLE at 120 and 240 mg of total polyphenols per kg oil and concluded that the consumption of fries pan-fried in the enriched oils could increase to 1.4-, 2.2-, and 1.5-fold tocopherols, phytosterols, and squalene intake compared to those prepared in the non-supplemented oil. Thus, these corroborated the findings from the present work, OLE increased the oxidative stability of palm oil.

The palm kernel oil sample containing 94 mgOLE.kg^{-1} of free OLE had the highest oxidative stability among all samples, reaching 14.28 h, showing similarity to the oxidative stability promoted by BHT ($p > 0.05$). Furthermore, the samples containing nanoparticles at 141 $mg_{OLE}.kg_{oil}^{-1}$ and free OLE at 47 mgOLE.kg^{-1} (13.8 h) were also statistically similar, meaning that the olive leaves extract significantly impacted the preservation of lipid oxidation.

3.3.2. Schaal oven test and PARAFAC analisys

Palm kernel oil was selected based on the Rancimat results to be evaluated by the Schaal oven test. The PARAFAC chemometric tool was applied using three factors for the tensor deconvolution (Gonçalves et al., 2018; Vieira & Regitano-D'Arce, 1998). In Fig. 7, the scores, loadings and spectral mode loadings obtained for each factor in the PARAFAC method are presented. Fig. 8 presents the UV–Vis spectrum of BHT in isooctane.

As may be observed from the results achieved by PARAFAC shown in Fig. 7 (a), the scores from Factor 1 indicated that the oil sample without antioxidant and the sample containing 150 $mg_{NP}.kg_{oil}^{-1}$ of nanoparticles were closely similar. In contrast, the oil samples with nanoparticles at 300 $mg_{NP}.kg_{oil}^{-1}$ are identical to oils with BHT at 300 $mg_{BHT}.kg_{oil}^{-1}$. The loadings relative to the spectral mode in Factor 1 (Fig. 7 c) indicated that this factor may be associated with primary oxidation products (monoene

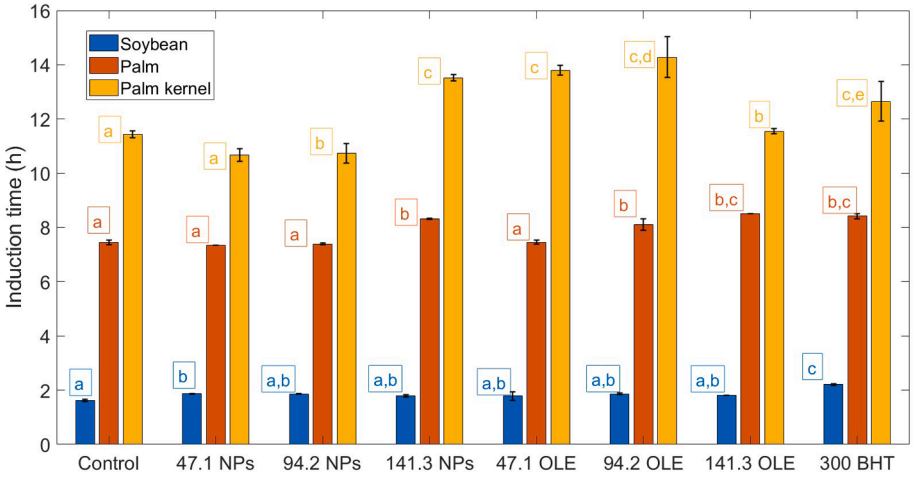

Fig. 6. Induction time determined by Rancimat for soybean, palm and palm Kernel oils containing OLE, OLE-loaded nanoparticles (both at 47, 94, and 141 $mg_{OLE}.kg_{oil}^{-1}$), BHT (at 300 $mg.kg_{oil}^{-1}$), and the control sample (no antioxidant added).[a,b]Different letters on the bars indicate a significant difference ($p < 0.05$) by Tukey's test. Comparisons were made between the different treatments for each oil type separately.

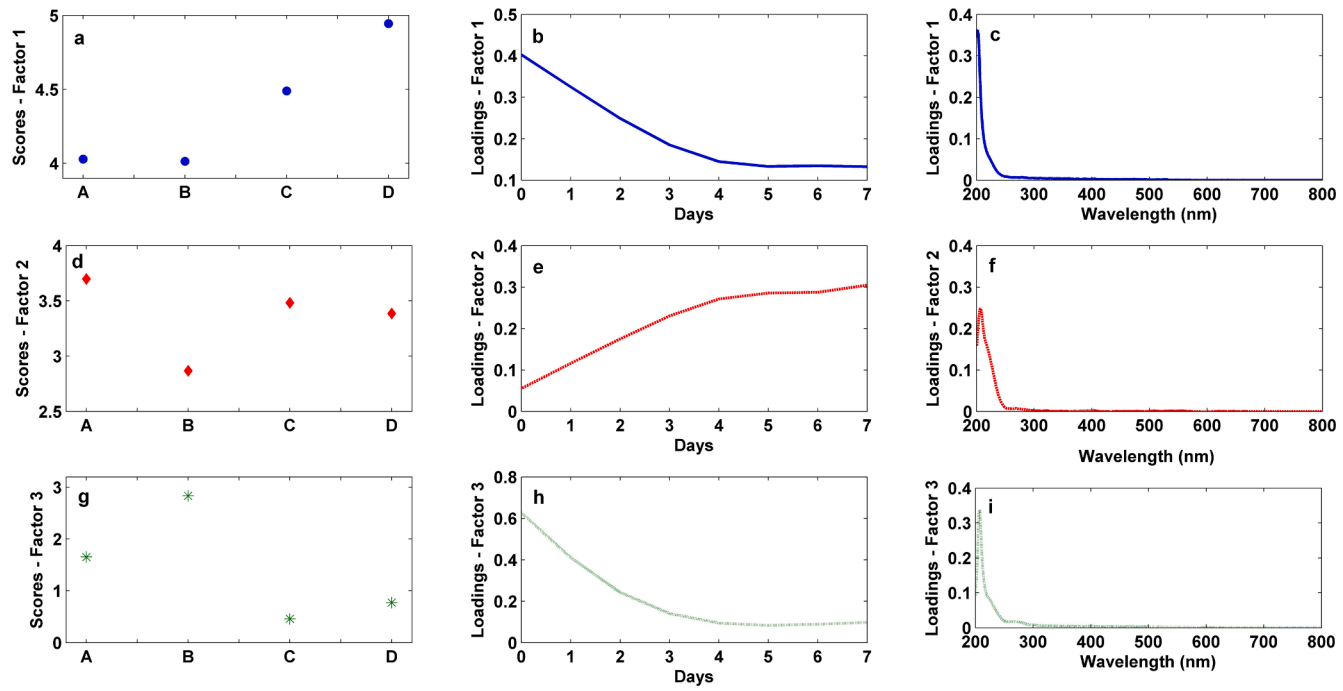

Fig. 7. PARAFAC results. Factor 1: (a) scores; (b) loadings relative to the storage time (days); (c) spectral mode loadings. Factor 2: (d) scores; (e) loadings relative to the storage time (days); (f) spectral mode loadings. Factor 3: (g) scores; (h) loadings relative to the storage time (days); (i) spectral mode loadings.

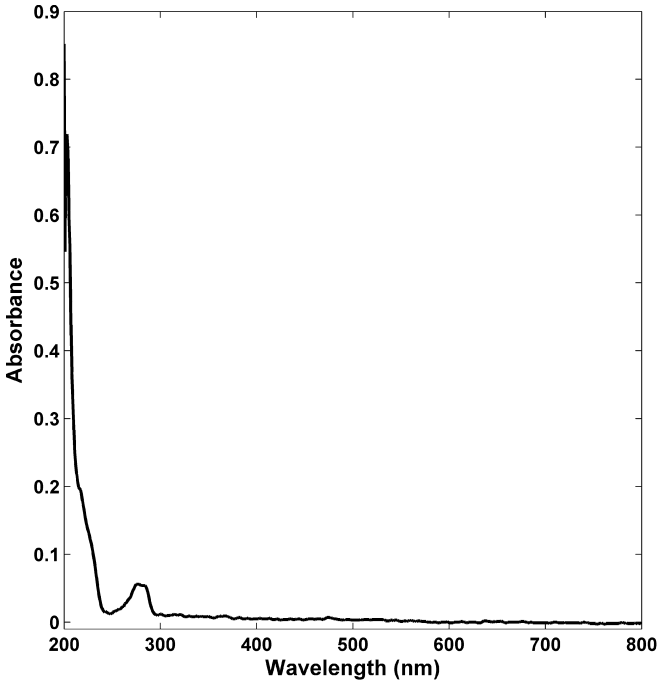

Fig. 8. UV–Vis spectrum of BHT in isooctane.

190 nm, α-ketone acid 210 nm, diene 220–230 nm, aldehyde ketone 220–250 nm) (Gonçalves et al., 2018; Vieira & Regitano-D'Arce, 1998). According to the loadings of storage time in Factor 1 (Fig. 7 b), these concentrations of oxidation products decreased over the days of exposure to temperature and could not be detected after the fourth day.

For the scores from Factor 2 (Fig. 7 d) it was possible to infer that treatments with 300 $mg_{NP}.kg_{oil}^{-1}$ and 300 $mg.kg_{oil}^{-1}$ BHT also presented similar effects on the samples. On the other hand, the oil sample with nanoparticles at a concentration of 150 $mg_{NP}.kg_{oil}^{-1}$ had the opposite behavior, which suggests that this concentration may have caused a pro-oxidant effect (Gonçalves et al., 2018; Vieira & Regitano-D'Arce, 1998). The loadings related to the spectral mode in Factor 2 (Fig. 7 f) referred to oxidation products formed over the exposure of the sample to 60 °C (loadings related to the days of analysis in Factor 2 - Fig. 7 e). These are oxidation products related to the compounds α,β ethylene (310 – 330 nm), triene (265 – 270 nm); ketonic aldehyde (265 – 280 nm), β-diketone (274 nm), α-diketone (280 nm) and α-ketoaldehyde (282 nm).

Factor 3 was also characterized by similarities between the treatments 300 $mg_{NP}.kg_{oil}^{-1}$ and 300 $mg.kg_{oil}^{-1}$ BHT and the opposite behavior for the treatment 150 $mg_{NP}.kg_{oil}^{-1}$ (Factor 3 scores in Fig. 7 g). Fig. 7 (h), which describes the loadings related to the storage time in Factor 3, showed that the concentration of the constituent responsible for this factor decreased over the exposure days. When evaluating the loadings related to the spectral mode in Factor 3 (Fig. 7 i), it was observed that it deals with the spectral profile of antioxidants, corroborating the spectrum of BHT in Fig. 8.

4. Conclusions

The proposed method efficiently extracted/encapsulated olive leaf extract using the one-step procedure, leading to the formation of zein nanoparticles containing olive leaf extract (OLE). FTIR analysis indicated the presence of interactions between the extracted compounds, while DSC/TGA demonstrated an increase in the thermal stability of the extract. Higher antioxidant activity was found for free OLE when compared to the OLE-loaded nanoparticles. No anti-inflammatory activity was found in the evaluated concentration range (up to 400 $\mu g_{OLE}.mL^{-1}$), and only lung cancer and gastric carcinoma were affected by free OLE. The antioxidant capacity of free and encapsulated OLE were compared to BHT, a known synthetic antioxidant. When added to soy, palm, and palm kernel oils, Rancimat significantly improved the oxidative stability of palm kernel oil due to its fatty acid composition. The Schaal oven test further investigated palm kernel oil, and the UV–Vis spectra data were evaluated by the PARAFAC chemometric method, revealing equivalent stability for BHT and nanoencapsulated OLE at the same concentrations.

CRediT authorship contribution statement

Amarilis Santos de Carvalho: Conceptualization, Investigation, Writing – original draft. **Anielle de Oliveira:** Investigation, Writing – original draft. **Thaysa Fernandes Moya Moreira:** Investigation, Writing – original draft. **Luis Gustavo Médice Arabel Costa:** Investigation, Writing – original draft. **Gabrielle Donato Marcatto:** Investigation, Writing – original draft. **Andre da Silva Castilhos de Melo:** Investigation, Writing – original draft. **Odinei Hess Gonçalves:** Formal analysis, Supervision, Writing – review & editing. **Maria Inês Dias:** Investigation, Formal analysis, Writing – original draft. **Ricardo C. Calhelha:** Investigation, Formal analysis, Writing – original draft. **Lillian Barros:** Resources, Formal analysis, Writing – review & editing. **Patricia Valderrama:** Formal analysis, Writing – review & editing, Funding acquisition. **Lucio Cardozo Filho:** Resources, Supervision, Writing – review & editing. **Fernanda Vitória Leimann:** Project administration, Funding acquisition, Writing – review & editing.

Declaration of Competing Interest

The authors declare that they have no known competing financial interests or personal relationships that could have appeared to influence the work reported in this paper.

Data availability

Data will be made available on request.

Acknowledgments

This study was financed in part by the Coordenação de Aperfeiçoamento de Pessoal de Nível Superior - Brasil (CAPES) - Finance Code 001. The authors thank the "Central Analítica Multiusuário da UTFPR Campo Mourão" (CAMulti-CM) for the analyses. Authors thank to CNPq (process number 406966/2021-4, Chamada CNPq/MCTI/FNDCT N° 18/2021 - Faixa A - Grupos Emergentes, and process number 310052/2021-1 Chamada CNPq N° 4/2021 - Bolsas de Produtividade em Pesquisa – PQ). This research was funded by FCT- Foundation for Science and Technology, P.I., (FCT, Portugal) through national funds FCT/MCTES to CIMO (UIDB/00690/2020 and UIDP/00690/2020), SusTEC (LA/P/0007/2021) and UIDB/50006/2020; national funding by FCT, P.I., through the institutional scientific employment program-contract for R. C., M.I.D. and L.B. contracts.

Appendix A. Supplementary material

Supplementary data to this article can be found online at https://doi.org/10.1016/j.foodres.2023.113363.

References

Ahin, S. S., Sayım, E., & Bilgin, M. (2017). Effect of olive leaf extract rich in oleuropein on the quality of virgin olive oil. *Journal of Food Science and Technology, 54*(6), 1721–1728. https://doi.org/10.1007/s13197-017-2607-7

ANVISA, A. N. de V. S. (2019). *RESOLUÇÃO - RDC Nº 281, DE 29 DE ABRIL DE 2019*.

Azar, F. A. N., Pezeshki, A., Ghanbarzadeh, B., Hamishehkar, H., Mohammadi, M., Hamdipour, S., & Daliri, H. (2021). Pectin-sodium caseinat hydrogel containing olive leaf extract-nano lipid carrier: Preparation, characterization and rheological properties. *LWT, 148*, Article 111757. https://doi.org/10.1016/J.LWT.2021.111757

Bessada, S. M. F., Barreira, J. C. M., Barros, L., Ferreira, I. C. F. R., & Oliveira, M. B. P. P. (2016). Phenolic profile and antioxidant activity of Coleostephus myconis (L.) Rchb. f.: An underexploited and highly disseminated species. *Industrial Crops and Products, 89*, 45–51. https://doi.org/10.1016/j.indcrop.2016.04.065

Brand-Williams, W., Cuvelier, M. E., & Berset, C. (1995). Use of a free radical method to evaluate antioxidant activity. *LWT - Food Science and Technology, 28*(1), 25–30. https://doi.org/10.1016/S0023-6438(95)80008-5

Caballero, A. S., Romero-García, J. M., Castro, E., & Cardona, C. A. (2020). Supercritical fluid extraction for enhancing polyphenolic compounds production from olive waste extracts. *Journal of Chemical Technology & Biotechnology, 95*, 356–362. https://doi.org/10.1002/jctb.5907

Calliari, C. M., Campardelli, R., Pettinato, M., & Perego, P. (2020). Encapsulation of Hibiscus sabdariffa Extract into Zein Nanoparticles. *Chemical Engineering and Technology, 43*(10), 2062–2072. https://doi.org/10.1002/ceat.202000194

Chee, S. S., & Jawaid, M. (2019). The effect of bi-functionalized MMT on morphology, thermal stability, dynamic mechanical, and tensile properties of epoxy/organoclay nanocomposites. *Polymers, 11*(12). https://doi.org/10.3390/polym11122012

Chiou, A., Kalogeropoulos, N., Salta, F. N., Efstathiou, P., & Andrikopoulos, N. K. (2009). Pan-frying of French fries in three different edible oils enriched with olive leaf extract: Oxidative stability and fate of microconstituents. *LWT - Food Science and Technology, 42*(6), 1090–1097. https://doi.org/10.1016/J.LWT.2009.01.004

Clodoveo, M. L., Crupi, P., Annunziato, A., & Corbo, F. (2021). *Innovative Extraction Technologies for Development of Functional Ingredients Based on Polyphenols from Olive Leaves.*. https://doi.org/10.3390/foods11010103

Coppa, C. F. S. C., Rosim, R. E., Oliveira, C. A. F. D., Rodrigues, C. E. D. C, & Gonçalves, C. B. (2017). Extração de oleuropeína a partir de folhas de oliveira utilizando solvente hidroalcoólico. *Brazilian Journal of Food Technology, 20*. https://doi.org/10.1590/1981-6723.16916

Crizel, R. L., Hoffmann, J. F., Zandoná, G. P., Lobo, P. M. S., Jorge, R. O., & Chaves, F. C. (2020). Characterization of Extra Virgin Olive Oil from Southern Brazil. *European Journal of Lipid Science and Technology, 122*, 1–12. https://doi.org/10.1002/ejlt.201900347

da Rosa, G. S., Vanga, S. K., Gariepy, Y., & Raghavan, V. (2019). Comparison of microwave, ultrasonic and conventional techniques for extraction of bioactive compounds from olive leaves (Olea europaea L.). *Innovative Food Science & Emerging Technologies, 58*, Article 102234. https://doi.org/10.1016/J.IFSET.2019.102234

da Silva, P. S., Viell, F. L. G., Ineu, R. P., Bona, E., Dias, M. I., Ferreira, I. C. F. R., … Cardozo-Filho, L. (2022). Determination of an optimum extraction region for the recovery of bioactive compounds from olive leaves (Olea europaea L.) using green dynamic pressurized liquid extraction. *Brazilian Journal of Chemical Engineering.*. https://doi.org/10.1007/s43153-022-00268-w

Danielski, R., Mazzutti, S., Ferreira, S. R. S., Vitali, L., & Block, J. M. (2022). A non-conventional approach for obtaining phenolic antioxidants from red guava (Psidium guajava L.) by-products. *Journal of Food Processing and Preservation.*. https://doi.org/10.1111/jfpp.16502

D'Antuono, I., Kontogianni, V. G., Kotsiou, K., Linsalata, V., Logrieco, A. F., Tasioula-Margari, M., & Cardinali, A. (2014). Polyphenolic characterization of olive mill wastewaters, coming from Italian and Greek olive cultivars, after membrane technology. *Food Research International, 65*, 301–310. https://doi.org/10.1016/j.foodres.2014.09.033

de Almeida Pontes, P. V., Shiwaku, I. A., Maximo, G. J., & Batista, E. A. C. (2021). Choline chloride-based deep eutectic solvents as potential solvent for extraction of phenolic compounds from olive leaves: Extraction optimization and solvent characterization. *Food Chemistry, 352*, Article 129346. https://doi.org/10.1016/J.FOODCHEM.2021.129346

Deng, L., Li, Y., Feng, F., & Zhang, H. (2019). Study on wettability, mechanical property and biocompatibility of electrospun gelatin/zein nanofibers cross-linked by glucose. *Food Hydrocolloids, 87*, 1–10. https://doi.org/10.1016/J.FOODHYD.2018.07.042

de Souza Tavares, W., Pena, G. R., Martin-Pastor, M., & de Sousa, F. F. O. (2021). Design and characterization of ellagic acid-loaded zein nanoparticles and their effect on the antioxidant and antibacterial activities. *Journal of Molecular Liquids, 341*, Article 116915. https://doi.org/10.1016/j.molliq.2021.116915

Difonzo, G., Squeo, G., Pasqualone, A., Summo, C., Paradiso, V. M., & Caponio, F. (2020). The challenge of exploiting polyphenols from olive leaves: Addition to foods to improve their shelf-life and nutritional value. *Journal of the Science of Food and Agriculture, 101*, 3099–3116. https://doi.org/10.1002/jsfa.10986

do Prado Silva, J. T., da Silva, A. C., Geiss, J. M. T., de Araújo, P. H. H., Becker, D., Bracht, L., Leimann, F. V., Bona, E., Guerra, G. P., & Gonçalves, O. H. (2017). Analytical validation of an ultraviolet–visible procedure for determining lutein concentration and application to lutein-loaded nanoparticles. *Food Chemistry, 230*, 336–342. https://doi.org/10.1016/j.foodchem.2017.03.059

Elnahas, R. A., Elwakil, B. H., Elshewemi, S. S., & Olama, Z. A. (2021). Egyptian Olea europaea leaves bioactive extract: Antibacterial and wound healing activity in normal and diabetic rats. *Journal of Traditional and Complementary Medicine, 11*(5), 427–434. https://doi.org/10.1016/j.jtcme.2021.02.008

Erdogan, I., Demir, M., & Bayraktar, O. (2015). Olive leaf extract as a crosslinking agent for the preparation of electrospun zein fibers. *Journal of Applied Polymer Science, 132*(4). https://doi.org/10.1002/app.41338

Feng, S., Wang, D., Gan, L., Shao, P., Jiang, L., & Sun, P. (2020). Preparation and characterization of zein/pectin-based phytosterol nanodispersions and kinetic study of phytosterol release during simulated digestion in vitro. *LWT, 128*, Article 109446. https://doi.org/10.1016/j.lwt.2020.109446

Gonçalves, T. R., Rosa, L. N., Gonçalves, R. P., Torquato, A. S., Março, P. H., Marques Gomes, S. T., … Valderrama, P. (2018). Monitoring the Oxidative Stability of Monovarietal Extra Virgin Olive Oils by UV–Vis Spectroscopy and MCR–ALS. *Food Analytical Methods, 11*(7), 1936–1943. https://doi.org/10.1007/s12161-018-1149-6

González-Ortega, R., Faieta, M., di Mattia, C. D., Valbonetti, L., & Pittia, P. (2020). Microencapsulation of olive leaf extract by freeze-drying: Effect of carrier composition on process efficiency and technological properties of the powders. *Journal of Food Engineering, 285*, Article 110089. https://doi.org/10.1016/j.jfoodeng.2020.110089

Guimarães-Inácio, A., Francisco, C. R. L., Rojas, V. M., Leone, R. D. S., Valderrama, P., Bona, E., … Gonçalves, O. H. (2018). Evaluation of the oxidative stability of chia oil-loaded microparticles by thermal, spectroscopic and chemometric methods. *LWT - Food Science and Technology, 87*. https://doi.org/10.1016/j.lwt.2017.09.031

Hajjari, M. M., Golmakani, M.-T., Sharif, N., & Niakousari, M. (2021). In-vitro and in-silico characterization of zein fiber incorporating cuminaldehyde. *Food and Bioproducts Processing, 128*, 166–176. https://doi.org/10.1016/j.fbp.2021.05.003

Joseph, J. D., & Ackman, R. G. (1992). Capillary column gas chromatography method for analysis of encapsulated fish oil and fish oil ethyl esters: Collaborative study. *Journal Association of Official Analytical Chemists, 75*(3), 488–506.

Karavas, E., Ktistis, G., Xenakis, A., & Georgarakis, E. (2006). Effect of hydrogen bonding interactions on the release mechanism of felodipine from nanodispersions with polyvinylpyrrolidone. *European Journal of Pharmaceutics and Biopharmaceutics, 63*, 103–114. https://doi.org/10.1016/j.ejpb.2006.01.016

Leimann, F. V., Cardozo Filho, L., Sayer, C., & Araújo, P. D. (2013). Poly(3-hydroxybutyrate-co-3- hydroxyvalerate) nanoparticles prepared by a miniemulsion/solvent evaporation technique: effect of phbv molar mass and concentration. *Brazilian Journal of Chemical Engineering, 30*(2), 369–377. https://doi.org/10.1590/S0104-66322013000200014

Leimann, V. F., Gonçalves, O. H., Sorita, G. D., Rezende, S., Bona, E., Fernandes, I. P. M., … Barreiro, M. F. (2019). Heat and pH stable curcumin-based hydrophylic colorants obtained by the solid dispersion technology assisted by spray-drying. *Chemical Engineering Science, 205*(21), 248–258. https://doi.org/10.1016/j.ces.2019.04.044

Lemes, G. F., Marchiore, N. G., Moreira, T. F. M., Da Silva, T. B. V., Sayer, C., Shirai, M. A., Gonçalves, O. H., Gozzo, A. M., & Leimann, F. V. (2017). Enzymatically crosslinked gelatin coating added of bioactive nanoparticles and antifungal agent: Effect on the quality of Benitaka grapes. *LWT - Food Science and Technology, 84*, 175–182. https://doi.org/10.1016/j.lwt.2017.05.050

Li, H., Yao, W., Liu, Q., Xu, J., Bao, B., Shan, M., Cao, Y., Cheng, F., Ding, A., & Zhang, L. (2017). Application of UHPLC-ESI-Q-TOF-MS to Identify Multiple Constituents in Processed Products of the Herbal Medicine Ligustri Lucidi Fructus. *Molecules, 22*(5), Article 689. https://doi.org/10.3390/molecules22050689

Lins, P. G., Pugine, S. M. P., Scatolini, A. M., & de Melo, M. P. (2018). Invitro antioxidant activity ofolive leaf extract (Olea europaea L.) and its protective effect on oxidative damage in human erythrocytes. *Heliyon, 4*(9), Article e00805. https://doi.org/10.1016/j.heliyon.2018.e00805

Llorent-Martínez, E. J., Gouveia, S., & Castilho, P. C. (2015). Analysis of phenolic compounds in leaves from endemic trees from Madeira Island. A contribution to the chemotaxonomy of Laurisilva forest species. *Industrial Crops and Products, 64*, 135–151. https://doi.org/10.1016/j.indcrop.2014.10.068

Milinsk, M. C., Matsushita, M., Visentainer, J. V., Oliveira, C. C. D., & Souza, N. E. D. (2008). Comparative analysis of eight esterification methods in the quantitative determination of vegetable oil fatty acid methyl esters (FAME). *Journal of the Brazilian Chemical Society, 19*(8), 1475–1483. https://doi.org/10.1590/S0103-50532008000800006

Mohammadi, A., Jafari, S. M., Esfanjani, A. F., & Akhavan, S. (2016). Application of nano-encapsulated olive leaf extract in controlling the oxidative stability of soybean oil. *Food Chemistry, 190*, 513–519. https://doi.org/10.1016/j.foodchem.2015.05.115

Moreno, M. A., Orqueda, M. E., Gómez-Mascaraque, L. G., Isla, M. I., & López-Rubio, A. (2019). Crosslinked electrospun zein-based food packaging coatings containing bioactive chilto fruit extracts. *Food Hydrocolloids, 95*, 496–505. https://doi.org/10.1016/J.FOODHYD.2019.05.001

Mourtzinos, I., Anastasopoulou, E., Petrou, A., Grigorakis, S., Makris, D., & Biliaderis, C. G. (2016). Optimization of a green extraction method for the recovery of polyphenols from olive leaf using cyclodextrins and glycerin as co-solvents. *Journal of Food Science and Technology, 53*(11), 3939–3947. https://doi.org/10.1007/s13197-016-2381-y

Oliviero, M., Verdolotti, L., di Maio, E., Aurilia, M., & Iannace, S. (2011). Effect of Supramolecular Structures on Thermoplastic ZeinÀLignin Bionanocomposites. *Journal of Agricultural and Food Chemistry, 59*, 10062–10070. https://doi.org/10.1021/jf201728p

Pappas, V. M., Lakka, A., Palaiogiannis, D., Athanasiadis, V., Bozinou, E., Ntourtoglou, G., … Lalas, S. I. (2021). Optimization of Pulsed Electric Field as Standalone "Green" Extraction Procedure for the Recovery of High Value-Added Compounds from Fresh Olive Leaves. *Antioxidants, 10*, 1554. https://doi.org/10.3390/antiox10101554

Pascoli, M., de Lima, R., & Fraceto, L. F. (2018). Zein Nanoparticles and Strategies to Improve Colloidal Stability: A Mini-Review. *Frontiers in Chemistry, 6*(6), 1–5. https://doi.org/10.3389/fchem.2018.00006

Pinela, J., Barros, L., Carvalho, A. M., & Ferreira, I. C. F. R. (2012). Nutritional composition and antioxidant activity of four tomato (Lycopersicon esculentum L.) farmer' varieties in Northeastern Portugal homegardens. *Food and Chemical Toxicology, 50*(3–4), 829–834. https://doi.org/10.1016/j.fct.2011.11.045

Rikhtehgaran, S., Katouzian, I., Jafari, S. M., Kiani, H., Maiorova, L. A., & Takbirgou, H. (2021). Casein-based nanodelivery of olive leaf phenolics: Preparation, characterization and release study. *Food Structure, 30*, Article 100227. https://doi.org/10.1016/J.FOOSTR.2021.100227

Rivas, C. J. M., Tarhini, M., Badri, W., Miladi, K., Greige-Gerges, H., Nazari, Q. A., … Elaissari, A. (2017). Nanoprecipitation process: From encapsulation to drug delivery. *International Journal of Pharmaceutics, 532*(1), 66–81. https://doi.org/10.1016/j.ijpharm.2017.08.064

Rosa, L. N., Coqueiro, A., Março, P. H., & Valderrama, P. (2019). Thermal rice oil degradation evaluated by UV–Vis-NIR and PARAFAC. *Food Chemistry, 273*, 52–56. https://doi.org/10.1016/J.FOODCHEM.2018.03.065

Şahin, S., & Şamlı, R. (2013). Optimization of olive leaf extract obtained by ultrasound-assisted extraction with response surface methodology. *Ultrasonics Sonochemistry, 20*(1), 595–602. https://doi.org/10.1016/j.ultsonch.2012.07.029

Salta, F. N., Mylona, A., Chiou, A., Boskou, G., & Andrikopoulos, N. K. (2007). Oxidative Stability of Edible Vegetable Oils Enriched in Polyphenols with Olive Leaf Extract. *Food Science and Technology International, 13*(6), 413–421. https://doi.org/10.1177/1082013208089563

Santos, C. H. K., Baqueta, M. R., Coqueiro, A., Dias, M. I., Barros, L., Barreiro, M. F., … Leimann, F. V. (2018). Systematic study on the extraction of antioxidants from pinhão (araucaria angustifolia (bertol.) Kuntze) coat. *Food Chemistry, 261*, 216–223. https://doi.org/10.1016/J.FOODCHEM.2018.04.057

Sanz, M., Simón, B. F., Cadahía, E., Esteruelas, E., Muñoz, A. M., Hernández, T., Estrella, I., & Pinto, E. (2012). LC-DAD/ESI-MS/MS study of phenolic compounds in ash (Fraxinus excelsior L. and F. americana L.) heartwood. Effect of toasting intensity at cooperage. *Journal of Mass Spectrometry, 47*(7), 905–918. https://doi.org/10.1002/jms.3040

Sena, M. M., Trevisan, M. G., & Poppi, R. J. (2005). PARAFAC: uma ferramenta quimiométrica para tratamento de dados multidimensionais. Aplicações na determinação direta de fármacos em plasma humano por espectrofluorimetria. *Química Nova, 28*(5), 910–920.

Souza, K. C., Correa, L. G., da Silva, T. B. V., Moreira, T. F. M., de Oliveira, A., Sakanaka, L. S., … Shirai, M. A. (2020). Soy Protein Isolate Films Incorporated with Pinhão (Araucaria angustifolia (Bertol.) Kuntze) Extract for Potential Use as Edible Oil Active Packaging. *Food and Bioprocess Technology, 13*(6), 998–1008. https://doi.org/10.1007/s11947-020-02454-5

Thaipong, K., Boonprakob, U., Crosby, K., Cisneros-Zevallos, L., & Hawkins Byrne, D. (2006). Comparison of ABTS, DPPH, FRAP, and ORAC assays for estimating antioxidant activity from guava fruit extracts. *Journal of Food Composition and Analysis, 19*(6–7), 669–675. https://doi.org/10.1016/j.jfca.2006.01.003

Vashisth, V., Nigam, K. D. P., & Kumar, V. (2021). Design and development of high shear mixers: Fundamentals, applications and recent progress. *Chemical Engineering Science, 232*, Article 116296. https://doi.org/10.1016/J.CES.2020.116296

Vieira, T. M. F. S., & Regitano-D'arce, M. A. B. (1998). Stability of oils heated by microwave: UV-spectrophotometric evaluation. *Food Science and Technology, 18*(4), 433–437. https://doi.org/10.1590/S0101-20611998000400015

Wang, L., & Zhang, Y. (2019). Heat-induced self-assembly of zein nanoparticles: Fabrication, stabilization and potential application as oral drug delivery. *Food Hydrocolloids, 90*, 403–412. https://doi.org/10.1016/J.FOODHYD.2018.12.040

Wu, Z., Ferreira, D. F., Crudo, D., Bosco, V., Stevanato, L., Costale, A., & Cravotto, G. (2019). Plant and Biomass Extraction and Valorisation under Hydrodynamic Cavitation. *Processes, 7*, 965–984. https://doi.org/10.3390/pr7120965

Zago, L., Squeo, G., Bertoncini, E. I., Difonzo, G., & Caponio, F. (2019). Chemical and sensory characterization of Brazilian virgin olive oils. *Food Research International, 126*, Article 108588. https://doi.org/10.1016/J.FOODRES.2019.108588

Zhao, Y., & Sun, Z. (2017). Effects of gelatin-polyphenol and gelatin–genipin cross-linking on the structure of gelatin hydrogels. *International Journal of Food Properties, 20*(sup3), S2822–S2832. https://doi.org/10.1080/10942912.2017.1381111

Zhu, Y., Sun, X., Ding, J., Fan, F., Li, P., Xia, J., … Fang, Y. (2021). Physicochemical and functional properties of a novel xanthan gum-lysozyme nanoparticle material prepared by high pressure homogenization. *LWT, 143*, Article 111136. https://doi.org/10.1016/j.lwt.2021.111136

Žugčić, T., Abdelkebir, R., Alcantara, C., Collado, M. C., García-Pérez, J. V., Meléndez-Martínez, A. J., … Barba, F. J. (2019). From extraction of valuable compounds to health promoting benefits of olive leaves through bioaccessibility, bioavailability and impact on gut microbiota. *Trends in Food Science & Technology, 83*, 63–77. https://doi.org/10.1016/J.TIFS.2018.11.005